

ZJ Liu
MW Anderson
GM Gu
GJ King

Apoptosis in the regenerate produced by mandibular osteodistraction in the mature rat*

Authors' affiliations:

Z.J. Liu, M.W. Anderson, G.M. Gu, G.J. King,
Department of Orthodontics, University of
Washington, Seattle, WA, USA

Correspondence to:

Dr Z.J. Liu
Department of Orthodontics, Box 357446
University of Washington
Seattle, WA 98195, USA
Tel.: (206)616-3870
Fax: (206)685-8163
E-mail: zjliu@u.washington.edu

Dates:

Accepted 7 September 2004

To cite this article:

Orthod Craniofacial Res **8**, 2005; 41–51
Liu ZJ, Anderson MW, Gu GM, King GJ:
Apoptosis in the regenerate produced by
mandibular osteodistraction in the mature rat

*A portion of this study was presented at the 82nd
General Session of the International Association
for Dental Research (IADR), Honolulu, USA,
March, 2004.

Copyright © Blackwell Munksgaard 2005

Structured Abstract

Authors – Liu ZJ, Anderson MW, Gu GM, King GJ

Objective – Little is known about the contribution of apoptosis to the formation of the regenerate in distraction osteogenesis. This study investigated the role of apoptosis in the regulation of osteogenesis in relation to mandibular distraction rate and recovery time.

Methods – One hundred and twenty-nine 3-month rats received unilateral mandibular ramus osteotomy and distraction device placement. After 3-day latency, these were distracted for 5 days. The slow group was distracted a total of 1 mm (0.2 mm/day), the moderate 2 mm (0.4 mm/day), the rapid 3 mm (0.6 mm/day), and the sham was not distracted (0.0 mm/day). Eight to nine rats from each group were killed at 6 (mid-distraction), 10 (early-consolidation), 24 (mid-consolidation) and 38 (late-consolidation) days following device placement. Baseline data were obtained from an additional eight rats killed at day 3 (end of latency). Sagittal sections (7 μ m) of the harvested hemi-mandibles were embedded in paraffin, double-stained with the DeadEnd™ Colorimetric TUNEL system for apoptotic cells and tartrate-resistant acid phosphatase for osteoclasts. Cell counts of apoptotic cells and osteoclasts (apoptotic or otherwise) were performed at 40 \times magnification using a calibrated grid at the middle regions of the caudal, central and rostral parts of the distraction gap. Counting reproducibility was verified as <13%.

Results – Counts from all three regions were combined because no significant regional difference was found. The majority of the fibrous matrix regenerate was seen at days 6 and 10 while osseous regenerate occurred mainly at days 24 and 38. Significantly higher levels of apoptotic activity were seen at day 24. Apoptotic osteoclasts also peaked at day 24.

Apoptotic cell numbers in the slow and moderate groups most closely followed the pattern of the sham in which the apoptosis activity peaked at days 10 or 24. However, those in the rapid group showed delayed peaks at days 24 or 38.

Conclusions – The transition from fibrous to osseous regenerate during mandibular distraction osteogenesis is accompanied by an increase in cell clearance via apoptosis. A slow to moderate distraction rate allows for the most typical pattern of bone healing while a rapid rate prolongs the healing process.

Key words: animal model; apoptosis; distraction osteogenesis; mandible; rat

Introduction

Distraction osteogenesis has become a prevalent mean to correct a variety of craniofacial abnormalities. This innovative technique utilizes strain manipulations to extend the potential of bone healing and regeneration beyond its normal level thus stimulating the bone formation. During distraction osteogenesis, new bone forms and undergoes rapid remodeling through the processes of the recruitment, differentiation and proliferation of osteogenic cells (1). On the contrary, apoptosis or programmed cell death also contributes greatly to the formation of the regenerate during distraction osteogenesis (2–5). Apoptosis may govern the removal of redundant callus and control the tissue integrity of the regenerate (3).

Apoptosis is involved in most bone cell types including osteoprogenitors, fibroblasts, chondroblast, osteoblasts, osteoclasts and osteocytes (6–9). As an important cellular mechanism, apoptosis has been demonstrated in alveolar bones and periodontal ligaments during normal resorption and remodeling (9), in response to stress-induced tissue changes such as orthodontic tooth movement (8, 10, 11). Transforming growth factor beta (TGF- β), fibroblast growth factor (FGF) and osteoprotegerin are molecular signals found to be important in these processes (12). During distraction osteogenesis, mechanical loading is thought to control tissue integrity by triggering apoptotic osteoblasts (13), and apoptotic activity positively relates to the amount of distraction strain or rate (4).

Understanding how the factors driving distraction (e.g. rate, rhythm and time course) relate to apoptosis during osteogenesis is crucial for improving osteodis-

traction procedures. Possible applications include the determination of the ideal distraction rate and consolidation period, and the temporally specific use of cell regulatory molecules (e.g. osteoprotegerin, TGF- β and FGF) in order to improve the bone regenerate quality, enhance the natural healing qualities of bone and inhibit chondrogenesis and fibrous union during distraction osteogenesis. As a time-dependent event in bone healing process, apoptosis may play different roles at specific periods of distraction (e.g. latency, distraction, early, middle or late consolidations). Few studies have been carried out on the role of apoptosis in distraction osteogenesis, and its relation to distraction rate and consolidation time. The purpose of the present study was to examine associations between osteodistraction rate and the prevalence of apoptotic cells at different time points. Because apoptosis has been shown to vary in relation to the quantitative and qualitative aspects of experimental stimuli such as mechanical stress *in vivo* and *in vitro* (2, 4, 10, 12), we hypothesize that apoptosis controls local tissue turnover by the removal of redundant cells. We further hypothesize that this function may be impaired or delayed by a rapid distraction rate.

Materials and methods

Animal handling and specimen preparation

This study used mandibular specimens collected from 135 three-month male rats. These rats received our standard mandibular distraction procedures, which have been described previously (14–17). In summary, the distraction device consists of a Leone jackscrew, two Luhr L-shaped microplates and four microcortical

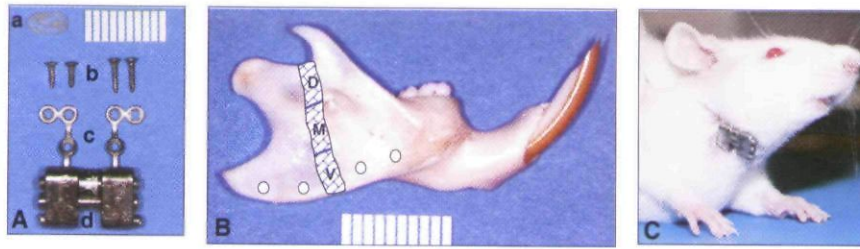


Fig. 1. (A) Components of distraction device. a, Acrylic wafer; b, self-tapping micro screws; c, Mini-plate welded to a jack screw; d, jaw screw. (B) The locations of the device placement (white dots) and distraction gap (hatched area). The gap were divided into ventral (V), middle (M) and dorsal (D) one-thirds. (C) The device in place during consolidation period.

self tapping screws (Fig. 1A). The anterior microplate was secured to the body of the mandible and the posterior one to the angle with an acrylic wafer as a support for the thin bone of the angle. After the device was placed, an osteotomy was performed from the sigmoid notch down to the inferior border between the two plates by using a diamond bur with copious irrigation (Fig. 1B). The muscle and skin incisions were closed in layers after a complete osteotomy was confirmed by activation the jackscrew. By convention, the surgery day was day 0, and the latency period lasted 3 days. Then, activation for mandibular distraction was performed once a day for 5 days. The consolidation period began at day 8, and terminated at day 38 (Fig. 1C).

These rats were randomly allocated into four groups, differing in distraction rate: 0.0 mm (sham), 0.2 mm (slow), 0.4 mm (moderate) and 0.6 mm (rapid), respectively. Eight to nine rats in each group were further randomized to sacrifice at the following four time points: day 6 (mid-distraction), 10 (early consolidation), 24 (middle consolidation) and 38 (late consolidation). After cardiac perfusion, harvested hemimandibles were fixed in 10% neutral buffered formalin for 72 h, decalcified by immersion in Immunocal and Decal-Arrest (Decal Chemical Co., Tallman, NY, USA) for 2 days and 20 min, respectively. The completion of the decalcification was checked by radiography. Finally, the specimens were embedded in paraffin and sectioned sagittally at the thickness of 7 μ m.

Immunohistochemical and histochemical stains

Apoptosis is most often identified by the terminal deoxynucleotidyl transferase (TdT) mediated dUTP-biotin nick end labeling (TUNEL) method. This method is very effective at identifying nuclear DNA fragmentation associated with apoptosis. In addition, we combined tartrate-resistant acid phosphatase (TRAP) stain with

the TUNEL, as a method for identifying osteoclasts. All stains were only applied to distracted hemimandibles.

The DeadEndTM Colorimetric TUNEL System (Promega, Madison, WI, USA) was used to detect apoptosis. Sections were deparaffinized in fresh xylene and washed twice in 100% ethanol for 5 min. Then rehydration was done with decreasing concentrations of ethanol (100, 95, 85, 70 and 50%) for 3 min at each time followed by immersion in 0.85% NaCl and phosphate buffered saline (PBS) for 5 min each. The slides were then fixed in 4% paraformaldehyde in PBS for 15 min and washed in PBS twice for 5 min each time. The permeabilization was then performed in 100 μ l of a 20 μ g/ml proteinase K solution for 15 min. After a 5-min wash in PBS, the slides were repeatedly fixed in 4% paraformaldehyde in PBS for 5 min. Equilibration in 100 μ l equilibration buffer was done for 5 min following another PBS wash. Labeling was performed by adding 100 μ l of TdT reaction mix to the tissue sections on the slides. Plastic coverslips were used to ensure even distribution and incubation was done for 60 min in a 37°C humidified chamber. The reaction was stopped by immersing slides in 2 \times Standard Saline Citrate for 15 min followed by three consecutive 5-min PBS washes. Immersion in 3% hydrogen peroxide for 3 min was done as the blocking step followed by another triple wash in PBS. Streptavidin HRP 100 μ l diluted 1:500 in PBS was then added followed by 30 min of incubation. A triple wash was then performed followed by the addition of 100 μ l DAB that was prepared immediately prior and allowed to incubate until a light brown background developed. Finally the slides were washed by immersing several times in deionized water. The positive control sections were treated with DNase I (Promega) prior to TUNEL staining, and the TdT was replaced by PBS for the negative controls.

To demonstrate the presence of osteoclasts, TRAP activity was shown using the protocol previously

described (8, 18). Slides were preincubated in 0.2 M Tris Buffer (pH 9.0) at 37°C for 1 h. Then, 5 ml pararosaniline stock solution was added to 0.2 g of NaNO₂ dissolved in 5 ml distilled water and mixed for 2 min (hexazotization). This solution was then added to 115 ml of 0.1 M acetate buffer followed by the addition of 0.287 g of sodium tartrate. 0.04 g of Naphthol-AS-TR phosphate was dissolved in 2 ml of dimethylformamide and this was added to the hexazotized pararosaniline-acetate buffer solution. The pH was adjusted to 5.0 with the addition of 4 N NaOH. The solution was immediately filtered into a glass dish for staining and the slides were incubated for 30 min at 37°C. The slides were rinsed with distilled water and allowed to air dry. Finally, the slides were counterstained with methyl green for 3–4 min followed by washing four times for 2 min in distilled water and then air drying. The slides were then dipped and agitated in a citrus-based clearing solvent and covered with VectaMount coverslips.

Image capturing and processing

Light microscopic photographic images were captured, optimized, and saved using a Spot RT camera running MetaVue software (Universal Imaging Co., Downingtown, PA, USA) under a Nikon Eclipse E400 light microscope (Nikon Co., Tokyo, Japan). A 1× image was first acquired for each hemimandible to show the entire distraction gap and adjacent bones. The three regions were selected from the dorsal, middle and ventral thirds

of the distraction gap (Fig. 2A). Each region was further captured separately at 4× (Fig. 2B). The central portion from each 4× image was further captured using a 40× lens (Fig. 2C) to ensure that the leading edge of the most novel cellular activity was included, because previously reported distraction studies have shown the middle region of regenerate to have the most cellular activity, the most TUNEL positive cells and the most mesenchymal progenitor cells (19, 20). The 60× images were also captured for the purpose of confirming morphological characteristics of apoptotic activity (Fig. 2D).

Regenerate classification

Each regenerate region was classified by the stage/type of ossification according to the major cell types and tissue components it contained, using a code system as follows: 1) hematoma; 2) fibrous; 3) mixed; 4) cartilaginous; 5) osseous.

Cell counting and statistical analysis

At the time of image capture, two 40× images were saved: one for general assessment and one with a calibrated grid for cell counting. A grid of 27 vertical lines and 20 horizontal lines was applied to the 115 mm² field creating 588 boxes of dimension 14 μm² and 567 total intersections (Fig. 3A).

Apoptotic osteoblasts, fibroblasts, mesenchymal cells and other cells were counted at the grid intersections

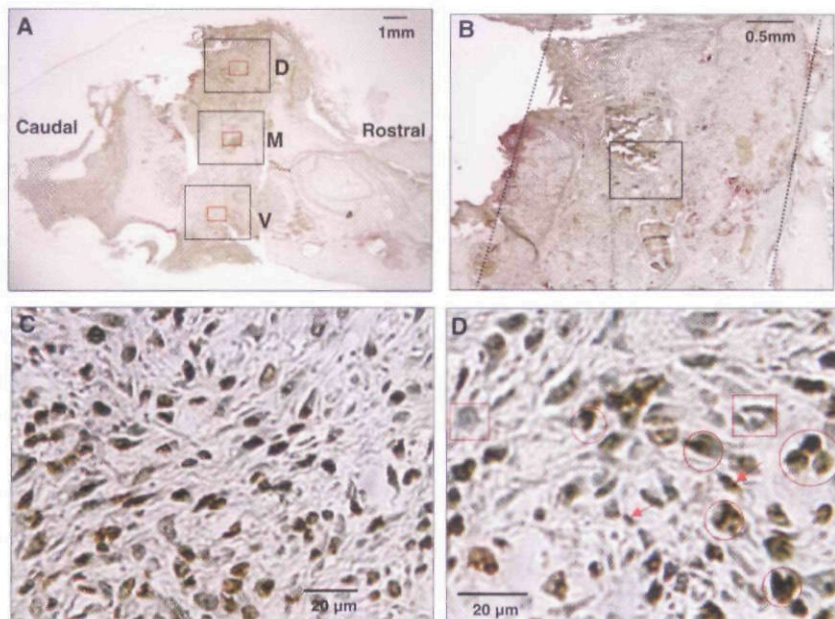
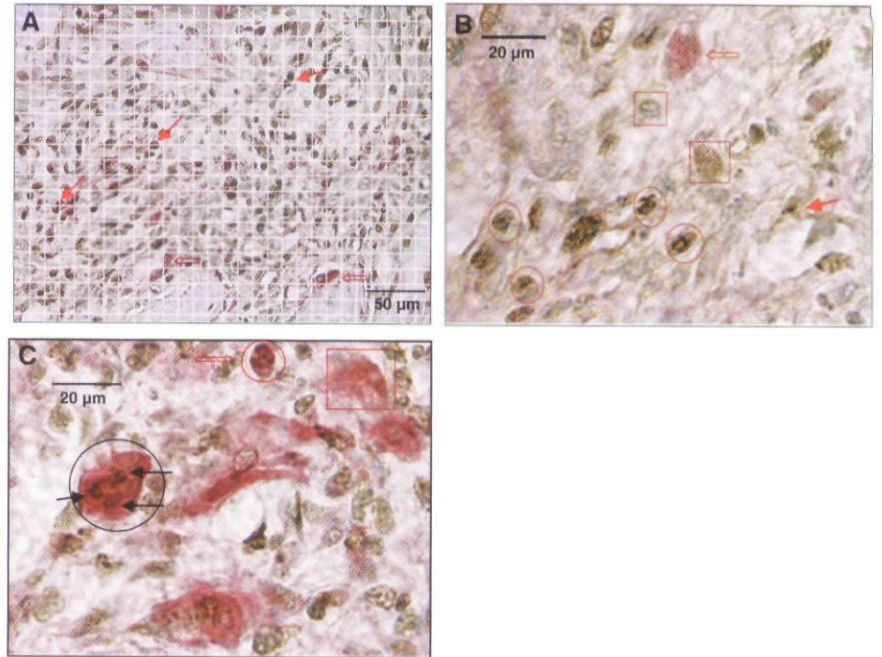


Fig. 2. (A) A 1× image of a specimen, the red boxes represent the areas that were captured as 4× images. (B) A 4× image of the dorsal part of A. The dotted lines approximate the osteotomy borders and the box indicates where the 40× image was captured. (C) A 40× image from the box of B. (D) A 60× image taken to confirm the 40× image results by showing morphological indications of apoptosis. The circled are TUNEL+ cells. Note the dark brown stain. The squares show cells that were stained lightly brown but were not counted. The arrows indicate small apoptotic bodies.

Fig. 3. (A) A 27×20 grid was superimposed on a $40\times$ image. A TUNEL-positive cell was only counted when it locates at the intersection of the grid (solid arrows). However, Osteoclasts were counted without grid consideration because of their size overlapping multiple grid intersection sites as two empty arrows indicate. (B) TUNEL+ (circled) osteoprogenitor cells (regenerate formers) were counted. They are typically $4\text{--}6\ \mu\text{m}$ in diameter, rounded to ovoid and dark brown in color. Cells in light brown or dark green (squared) were considered TUNEL- without counting. The solid and empty arrows indicate an apoptotic body and a TUNEL- osteoclast, respectively. (C) The large and small circles indicate TUNEL/TRAP double positive staining apoptotic osteoclasts with multi- and mono-nuclei, respectively. The square indicates a TUNEL- osteoclast. Solid arrows indicate pyknotic nuclei. Condensed and marginating chromatin is indicated by the empty arrow pointing to the smaller mononuclear osteoclast.



only. These potential osteoprogenitor cells were typically $4\text{--}6\ \mu\text{m}$ in diameter, rounded to ovoid and dark brown in color (Fig. 3B). Cells whose outer margins touched the point of intersection were considered as being at the intersection as were cells that had the grid intersection transposed directly over any part of the cell body. However, apoptotic and non-apoptotic osteoclasts were counted without the grid consideration (Fig. 3C).

For both osteoprogenitor cells and osteoclasts, condensed chromatin, pyknotic nuclei and chromatin margination were considered signs of apoptosis when present with dark brown staining, whereas light brown staining was ignored as it is most likely evidence of the TUNEL stain binding to naturally occurring 3'-OH ends (Fig. 2D and 3B). Furthermore, light and diffuse pink staining without clear cell borders was also ignored because it is most likely a result of acid phosphatase diffusing outside of an osteoclast (Fig. 3C).

Cell counting was performed manually and a reproducibility error of $<13\%$ was established by recounting 25 randomly selected images. These counts were then compared with the original counts with Dahlberg's equation ($\sqrt{\sum d^2/2n}$) where d is the difference in the count totals of the selected samples and n is the number of samples used, 25 in this case (21). To reduce the number of false positives in sampling slides, apoptotic cells in each negative control slide were counted in the same way, and this number was subtracted from the corresponding sampling slide.

Preliminary statistical analysis did not show regional difference, thus counts from the three selected regions (dorsal, middle and ventral) were combined. Both apoptotic and non-apoptotic osteoclasts were combined as well. Non-parametric statistics was applied as the data distributed abnormally. The mean ranks were compared across time by Kruskal Wallis test, followed by Mann-Whitney test for pairwise comparisons between each two time points. Significance level was set at $p < 0.05$.

Results

General examination and types of ossification

Of the original sample of 147 rats, six died from complications involved with the procedure and six of the surviving rats did not produce adequate micro-sections for examination. While the vast majority of the slides were easily discernable, others had to be examined more closely for determining regenerate margins with original bone, orientation (i.e. dorsal vs. ventral) and the central regenerate zone especially for late day samples. In a few cases the regenerate was separated from the proximal bone which made it easy to identify but raised questions as to the integrity of the regenerate. Despite these, the majority of the slides showed a clear demarcation between regenerate and originally adjacent bones and the dorso-ventral position was

Table 1. Classifications of the regenerates at five time points

Time	n	Hematoma	Fibrous	Mixed	Cartilaginous	Osseous
Day3	8	8 (100%)	0	0	0	0
Day 6	31	26 (83.9%)	5 (16.1%)	0	0	0
Day 10	31	0	26 (83.9%)	3 (9.7%)	2 (6.4%)	0
Day 24	33	0	12 (36.4%)	8 (24.2%)	8 (24.2%)	4 (12.1%)
Day 38	32	0	11 (34.4%)	4 (12.55)	2 (6.3%)	15 (46.9%)
Total	135	34 (25.2%)	54 (40.0%)	15 (11.1%)	12 (8.9%)	19 (14.1%)

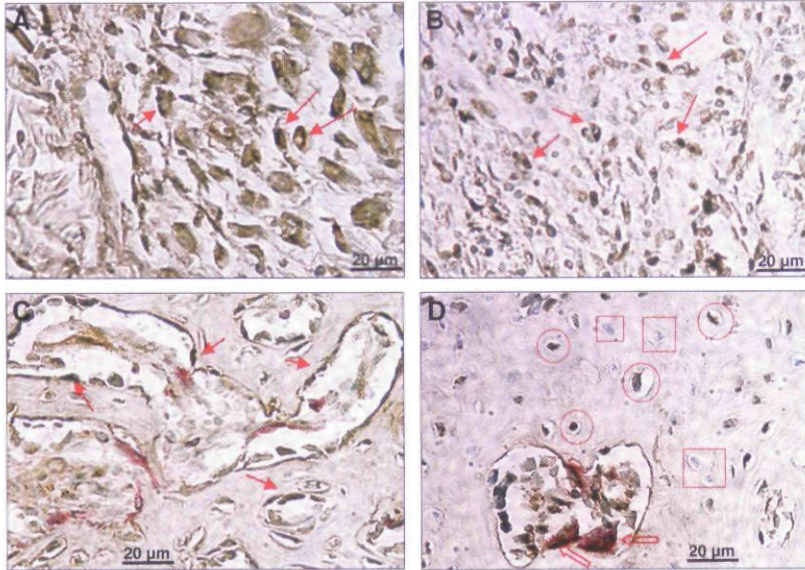


Fig. 4. (A) A 6-day distraction gap showing extensive hematoma. The fibrin clot and the beginning of the fibrous matrix can be seen in the extensively brown region (arrows). (B) A 10-day distraction gap showing fibroblasts that are apoptotic (arrows) and embedded in the wavy fibrous matrix. (C) A 24-day distraction gap showing intra-membranous ossification. Marrow spaces are shown where the heavy apoptotic activities occur (arrows). (D) A 38-day distraction gap showing progressive bone corticalization and remodeling (continuous sheet of lamellar bone). The circles and squares indicate small and round osteocytes in their lacunae with TUNEL+ and TUNEL- stains, respectively. Empty arrows indicate osteoclasts aligning along the boarder of the bone marrow.

determined by either the condyle or the device placement holes (located ventrally). Therefore, we were able to clarify the types of ossification in the regenerate at 4× with 40× used only to confirm.

Osseous and fibrous regenerate types were classified alone and in combination with each other and with chondrogenesis. The regenerate classification types varied greatly across different time points (Table 1). However, the distraction rates seemed to have less impact on this qualitative count (data not shown). All day 3 samples showed hematoma. Day 6 mainly presented hematoma (83.9%) with fibrin clot/edema surrounded by a pool of cells and embedded in the beginnings of a wavy fibrous background (Fig. 4A). Day 10 appeared similar but the collagen fibers were generally more distinct and organized, and aligned in the direction of the force vector. Various cells, presumably fibroblasts or pre-fibroblasts, were seen. These cells were embedded within fibers and in between fibers (Fig. 4B), thus this kind of regenerate was classified fibrous (83.9%). In a few cases, a small number of

islands of osseous tissue were seen. Day 24 was fibro-osseous for the most part with delicate islands of trabeculae that started at the margin with original bone and grew towards the center of the regenerate (Fig. 4C). Day 38 was often a continuous sheet of lamellar bone with osteocytes (46.9%) in lacunae and various cell types including osteoclasts in marrow spaces (Fig. 4D).

At both early and late time points, chondrogenesis (cartilaginous) occurred in some specimens, which was most often seen in combination with fibrous and/or osseous regenerate and appeared as an isolated island. The screw holes were sometimes non-geometric in shape and had a cellular presence similar to that in the regenerating bone, indicating a small degree of mobility in all directions (visible at 1×) of the device and compensatory bone remodeling.

Apoptotic activities

Apoptosis was readily observed in almost every sample. The majority of apoptotic cells were seen against a

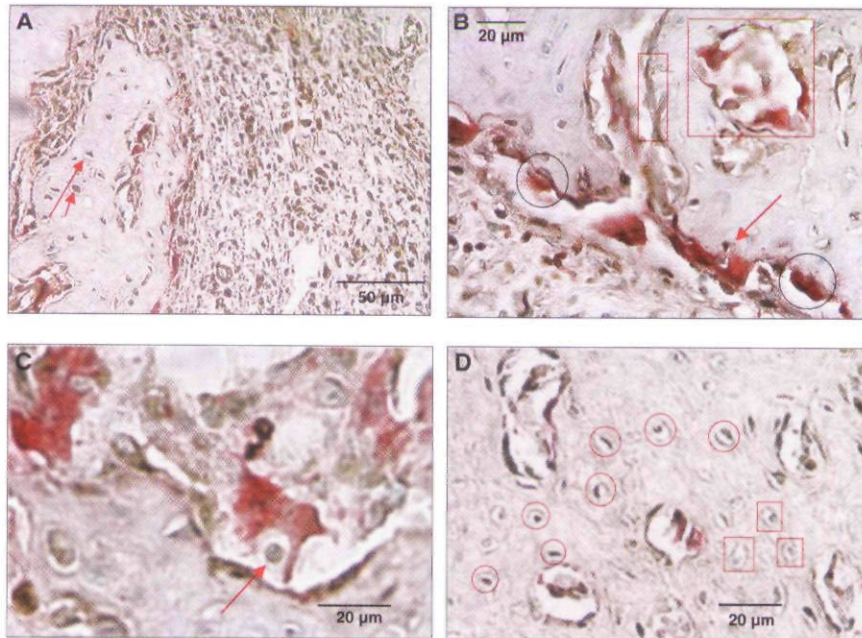


Fig. 5. (A) A 24-day regenerate showing the transition from fibrous to osseous and peak of apoptotic activities. The arrows indicate osteocytes. The regenerate is clearly half fibrous and half osseous. The majority of the apoptotic activity is occurring in the fibrous region. Again, the apoptotic cells are embedded in the wavy fibrous matrix. (B) Active osteoclast activities at the bone surfaces and within marrow spaces. The circles indicate osteoclasts that are adjacent to bone surfaces and appear to be trapping other cell from their proximity (arrow). The bone surfaces without osteoclast presence show elongated brown cellular material (rectangular). The square indicates osteoclast presence in a bone marrow. (C) An osteoclast in bone marrow shows phagocytosis. The arrow points to a cell that is completely within an engulfing osteoclast. (D) The original bone adjacent to the distraction gap showing apoptotic (circles) and non-apoptotic (squares) osteocytes.

fibrous background in both fibrous and fibro-osseous sections. A large quantity of apoptotic cells were seen at the margins of newly formed bone and within marrow spaces (Fig. 5A). Osteoclasts were also seen most frequently in these locations (Fig. 5B) and were observed actively phagocytosing apoptotic cells (Fig. 5C). Apoptotic osteocytes were also seen, particularly in the original bone adjacent to the osteotomy and in 38-day intramembraneous regenerate bone (Fig. 5D).

Figure 6 shows apoptotic activities of 'regenerate formers', chondrocytes and osteoclasts across four time points when all rates were combined. TUNEL+ cells in the regenerate peaked at day 24 significantly for 'regenerate formers' ($p < 0.05$, Fig. 6A), chondrocytes ($p < 0.01$, Fig. 6B) compared with the other three time points (6, 10 and 38 days). There is also a clear trend that both apoptotic osteoclasts and total osteoclasts (apoptotic and non-apoptotic) peaked at day 24 although no statistical significance was found (Fig. 6C and D).

To further examine the effects of different distraction rates, the time-course apoptotic activities of 'regenerate formers' at each rate were examined and the results are shown in Fig. 7. The peak of apoptosis varied greatly dependent upon the rates. The apoptotic activity of the

sham rate surpassed the baseline (day 3) at day 10 (peak) and lasted till day 24, then dropped down to a level close to the baseline. This time-course curve shifted right when the slow rate was applied, showing a significant peak at day 24 ($p < 0.05$), instead of day 10. The time-course curve of the moderate rate was similar to the sham that spread out over the 10- and 24-day time periods with much higher TUNEL+ cell counts compared to the sham (median: ~ 60 versus ~ 40), and was down to the similar level of the baseline at day 38. At the rapid rate, the time period with higher counts of TUNEL+ cells further extended to day 38 and reached a peak at this time point.

Discussion

This study was performed as a part of a larger study that has used rats to study distraction osteogenesis in a way that allows the larger sample size and produces appropriate statistical power to characterize the properties of the regenerates and the mechanisms of cellular regulations by different distraction rates and time points. If it is found, as published elsewhere (22–24), that a slow or moderate rate of distraction promotes

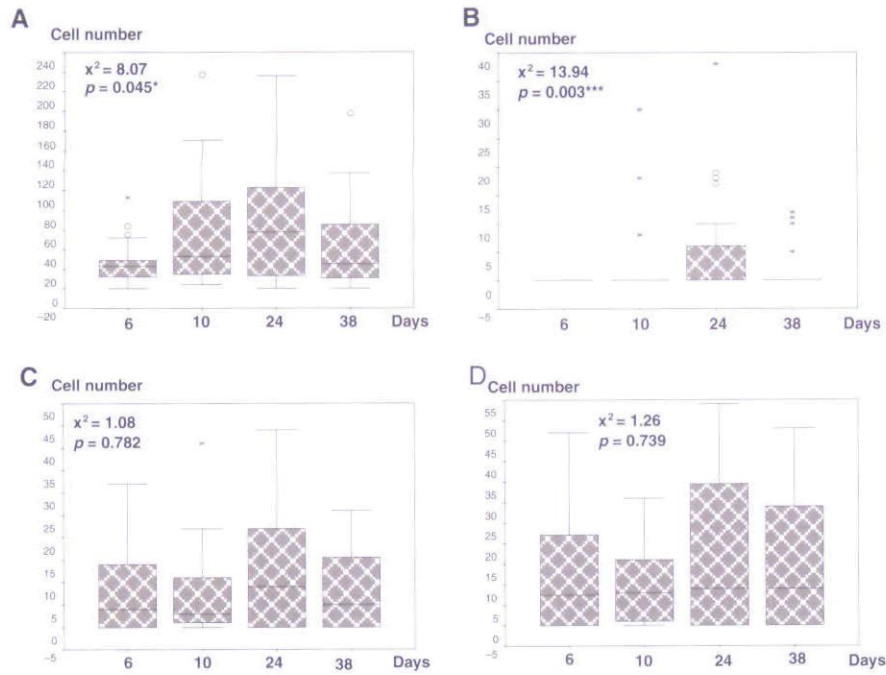


Fig. 6. Boxplots of counted cell numbers across the time showing the time-course effects on different cell types. (A) Apoptotic cells of 'regenerate formers' including fibroblasts, osteoclasts, mechenchymal cells and other cell types. (B) Apoptotic chondrocytes. (C) Apoptotic osteoclasts. (D) Total osteoclasts. Upper and lower limits of box represent 75th and 25th percentile, respectively. Horizontal line within each box represents median. Marks outside box represent outliers (small circles, 1.5-3 of box length) and extremes (asterisks, >3 of box length). All cell types show the peaks at day 24 with statistically significance for cells of 'regenerate former' ($p < 0.05$) and chondorcytes ($p < 0.01$).

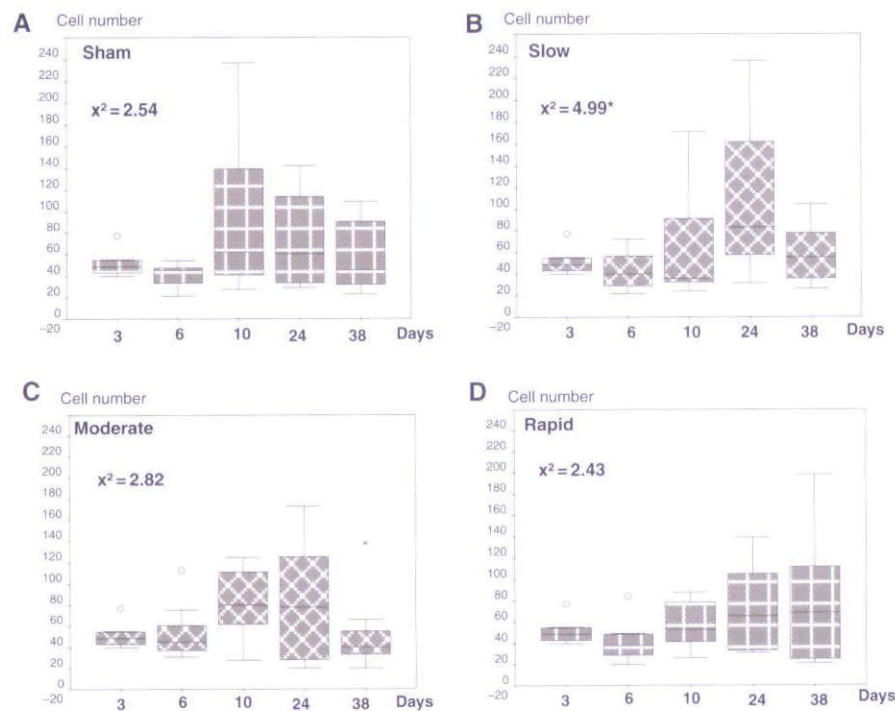


Fig. 7. Boxplots of counted 'regenerate formers' numbers at each distraction rate across the time showing the rate effects. (A) Sham. (B) Slow. (C) Moderate. (D) Rapid. Note that the peak of apoptosis and time-course curves varied greatly dependent upon the rates. See Fig. 6 for all captions.

the most effective bone regeneration sequence with regards to apoptosis, osteoclast activity, etc., it may provide strong evidence to guide an appropriate clinical application of the distraction and to induce possible timely intervention, such as growth factors, to expedite the regenerating process. While considerations must be made with regard to the differences between the models and between the protocols, overall

patterns of regeneration and cellular mechanisms like apoptosis and osteoclast activities can be observed, analyzed and translated in a similar manner.

The reliability of the current method for *in vivo* staining to identify cell death has been questioned (3). It has been said to be hyper-sensitive resulting in overestimation of apoptotic activity (25). Other studies using this method have noted this possibility but have

insisted that despite its deficiencies as a true measure of apoptosis, the data provided can still be informative when viewed as relative rates (8). Homeostatic negative controls (peripheral nerve and brain) as well as intact cortical bone negative controls in other studies have showed little positive TUNEL staining indicating that apoptosis staining can reliably reflect the cell death situation of a given tissue (26). As only very few or no TUNEL+ cells were found in the negative-control slides, the present results confirmed the effectiveness of TUNEL staining as an indicator of relative rates by counting only cells that stained dark brown and had histologic indication of apoptosis i.e. pyknotic chromatin, disrupted membrane, apoptotic bodies, spheroidal appearance, etc., and by subtracting any counts from corresponding negative controls. Therefore, we were able to reduce the number of false positives created by light brown staining of diffuse and naturally occurring 3'-OH ends.

The regenerate and its time-course sequence in the present study showed ultrastructural and histological similarities to what are considered typical in distraction osteogenesis (27). After the latency period, a fibrin clot formed with mesenchymal cells at margins. After distraction, this was replaced by granulation tissue and proliferating mesenchyme-like cells. Apoptotic fibroblast-like cells embedded in wavy collagen fibers were seen adjacent to the original bone at day 10 and 24, and woven delicate trabeculae grew in the direction of tension and gradually mineralized. All of these descriptions coincide with what was seen in other large animal studies (4, 5, 27).

A previous study showed that the regenerate at day 6 and 10 had a significant decrease in bone density while day 24 and 38 samples had slightly increased bone density over the control side (22). Furthermore, the sequential histomorphometric analysis of mineral apposition rate (24), fractal analysis (28) and trabecular organization analysis (23) in the regenerate demonstrated consistently that the activity of bone formation peaked at day 24. This suggests that the peaks in apoptosis and osteoclast activity at day 24 contribute to the rapid increase in bone formation and remodeling which occur simultaneously during distraction osteogenesis (13, 29). Therefore, day 24 may be the time that marks the transition of the regenerate from fibrous to osseous. Being most often a fibro-osseous mix, the day-24 regenerate in the present study possessed 1) a high

proportion of areas with fibrous background; 2) a large number of marrow spaces; 3) a greater surface area of bone margins due to the irregular extensions of the newly formed trabeculae; 4) the greatest presence of osteoclasts; 5) the highest occurrence of isolated cartilage island. These five factors led to apoptotic activity peaking at this time point.

The previous study also indicated that slow and moderate distraction rates led to the regenerate with the stronger biomechanical and histological properties, while having similar bone density readings to rapidly distracted specimens (30). The present study showed the most characteristic pattern of apoptotic and osteoclast activities in these rate groups. Therefore, slow and moderate rates are associated with the regenerate that is more mechanically desirable, and this structural improvement is not related to bone density but more likely is a result of a more organized bone. Such an improved organization comes from the efficiency of the cellular processes involved in remodeling. This efficiency in the case of apoptosis and osteoclast activity appears to peak in day 24 (middle consolidation) when a slow or moderate distraction rate is applied. One possible explanation for this correlation is the improved neovascularization of the fibrous zone seen with slow or moderate distraction. More angiogenesis results in more efficient delivery and dispersal of bone repair cells as well as chemical signals like insulin-like growth factor -1 (IGF-1) and fibroblast growth factor -2 (FGF-2) that have been shown to have a positive influence on consolidation and thus are likely to play a role in controlling apoptosis and osteoclast presence and activity (31, 32). Basic fibroblast growth factor (b-FGF) has been shown to be prevalent in the remodeling phase of distraction osteogenesis and especially in active osteoclasts (33). It is thought that b-FGF is stored in the matrix and released in cases of bone fracture. Clearly, b-FGF whether released from damaged bone or apoptotic cells, is an essential molecular mechanism for controlling regenerate integrity by regulating the actions of osteoclasts (34). The TGF- β has been shown to be prevalent in the osteoid seam and is known to cause apoptosis of osteoclasts (35). The osteoid seam, being near the first zone of regenerate bone to be completed, may be releasing TGF- β locally so that osteoclasts will self-terminate or decrease their activity when they are no longer needed. The b-FGF which stains heavily in the fibrous stroma of the regenerate,

may be activating osteoclasts and bone forming cells to form and remodel bone at the leading edge. Immunohistochemical analyses for these factors have been performed on regenerate bones that exhibited intramembranous ossification and rare sites of cartilaginous metaplasia similar to the present samples.

Osteoclasts recruited for orthodontic tooth movement have been shown to be cleared by apoptosis that is at its greatest levels within marrow spaces and on bone borders (8, 12). This phenomenon was also observed in the present study. As the morphology of the regenerate produced at day 24 by the slow and moderate rates was such that marrow spaces and bone borders were maximized, it elevates apoptosis and osteoclasts. Because apoptosis and osteoclast activity are integral in creating a regenerate that shows well organized and mechanically optimal, we speculate that chemical or biological signals may be added or removed to strengthen or improve the cellular process occurring at day 24 (mid-consolidation).

Osteoclasts are multinucleated cells derived from granulocyte-monocyte stem cells located in hematopoietic bone marrow. It has been suggested that osteoclasts are attracted to resorption sites by signals released from dying bone cell (9, 36). It has been proven that endothelial monocyte activating polypeptide II (EMAP II) released from apoptotic cells attracts macrophages and a similar mechanism is likely to exist in osteoclasts. The present observation that apoptosis and osteoclast activity peak at the same time suggests that osteoclasts are at least partly responsible for apoptotic cell clearance (20). In the periodontal ligament space on the compressed side during orthodontic tooth movement, a peak in apoptosis was shown to be directly followed by high osteoclast activity and a sudden reduction in apoptotic material (11). It is thus intuitive that osteoclasts in the regenerate play a similar role as cell clearance specialists to remove apoptotic cells (5, 37). In this study elongated TUNEL-positive cells or bodies were seen in marrow spaces trapped between bone margins and TRAP+ cells. Elongated TRAP+ cells were also seen surrounding TUNEL+ cells that lined bone margins and marrow spaces. The elongation of TRAP+ cells may represent a morphological reaction to the high chemical gradient at the bone margins that controls remodeling and phagocytosis of the apoptotic material lining the bone (9). The elongated TUNEL+ cells or bodies may be

conglomerations of apoptotic bone forming cells, or the remains of osteoclasts that have removed the apoptotic material and have gone through apoptosis themselves thus producing no acid phosphatase and consequently no TRAP staining.

Conclusions

1. Apoptosis in mandibular distraction osteogenesis is characterized by a temporal peak at day 24, defined as mid-consolidation period.
2. Osteoclast activity, both apoptotic or otherwise, also peaks at mid-consolidation during distraction osteogenesis.
3. Regenerate composition transitions from fibrous to osseous with a timing that coincides with the peak in apoptotic and osteoclast activity.
4. A slow to moderate distraction rate promises the most typical pattern of bone healing while a rapid rate prolongs the healing process.
5. Increased distraction rate shows a positive correlation with increased apoptotic activity.

Acknowledgements: We would like to thank Ms Xian-Qin Bai and Noralyn Altases for their expertise for histology and general lab assistance. Thanks also go to Drs Norimasa Okafuji and Jayoung Shin, visiting scholars from Japan and Korea, respectively, for their help on animal experiments along with Ms Xian-Qin Bai. This study was supported by NIH grants PHS P60 13061 and T35 DE 07150.

References

1. Aronson J, Hogue WR, Flahiff CM et al. Development of tensile strength during distraction osteogenesis in a rat model. *J Orthop Res* 2001;**19**:64–9.
2. Meyer U, Wiesmann HP, Kruse-Losler B, Handschel J, Stratmann U, Joos U. Strain-related bone remodeling in distraction osteogenesis of the mandible. *Plast Reconstr Surg* 1999;**103**:800–7.
3. Li G, Dickson GR, Marsh DR, Simpson H. Rapid new bone tissue remodeling during distraction osteogenesis is associated with apoptosis. *J Orthop Res* 2003;**21**:28–35.
4. Meyer U, Meyer T, Wiesmann HP et al. Mechanical tension in distraction osteogenesis regulates chondrocytic differentiation. *Int J Oral Maxillofac Surg* 2001;**30**:522–30.
5. Rachmiel A, Rozen N, Peled M, Lewinson D. Characterization of midface maxillary membranous bone formation during distraction osteogenesis. *Plast Reconstr Surg* 2002;**109**:1611–20.
6. Lee FY, Choi YW, Behrens FF, DeFouw DO, Einhorn TA. Programmed removal of chondrocytes during endochondral fracture healing. *J Orthop Res* 1998;**16**:144–50.

7. Landry P, Sadasivan K, Marino A, Albright J. Apoptosis is coordinately regulated with osteoblast formation during bone healing. *Tissue Cell* 1997;**29**:413–9.
8. Noxon SJ, King GJ, Gu G, Huang G. Osteoclast clearance from periodontal tissues during orthodontic tooth movement. *Am J Orthod Dentofacial Orthop* 2001;**120**:466–76.
9. Boabaid F, Cerri PS, Katchburian E. Apoptotic bone cells may be engulfed by osteoclasts during alveolar bone resorption in young rats. *Tissue Cell* 2001;**33**:318–25.
10. Hamaya M, Mizoguchi I, Sakakura Y, Yajima T, Abiko Y. Cell death of osteocytes occurs in rat alveolar bone during experimental tooth movement. *Calcif Tissue Int* 2002;**70**:117–26.
11. Hatai T, Yokozeki M, Funato N et al. Apoptosis of periodontal ligament cells induced by mechanical stress during tooth movement. *Oral Dis* 2001;**7**:287–90.
12. Kobayashi Y, Hashimoto F, Miyamoto H et al. Force-induced osteoclast apoptosis in vivo is accompanied by elevation in transforming growth factor beta and osteoprotegerin expression. *J Bone Miner Res* 2000;**15**:1924–34.
13. Meyer T, Meyer U, Stratmann U, Wiesmann HP, Joos U. Identification of apoptotic cell death in distraction osteogenesis. *Cell Biol Int* 1999;**23**:439–46.
14. Connolly JP, Liu ZJ, Wang L et al. A custom mandibular distraction device for the rat. *J Craniofac Surg* 2002;**13**:445–50; discussion 450–2.
15. Baskin CR, Liu ZJ, King GJ, Maggio-Price L. Vascular leak syndrome of Sprague–Dawley rats in a mandibular distraction osteogenesis study. *Comp Med* 2003;**53**:207–12.
16. Liu ZJ, King GJ, Herring SW. Alterations of morphology and microdensity in the condyle after mandibular osteodistraction in the rat. *J Oral Maxillofac Surg* 2003;**61**:918–27.
17. King GJ, Liu ZJ, Kim AY, Bai XQ. Mineralization and microdensity in the regenerate following mandibular distraction in growing rats. *J Dent Res* 2003;**82**:1216.
18. Rody WJ Jr, King GJ, Gu G. Osteoclast recruitment to sites of compression in orthodontic tooth movement. *Am J Orthod Dentofacial Orthop* 2001;**120**:477–89.
19. Rachmiel A, Levy M, Laufer D. Lengthening of the mandible by distraction osteogenesis: report of cases. *J Oral Maxillofac Surg* 1995;**53**:838–46.
20. Li J, Hu J, Wang D, Tang Z, Gao Z. Biomechanical properties of regenerated bone by mandibular distraction osteogenesis. *Chin J Traumatol* 2002;**5**:67–70.
21. Dahlberg G. *Statistical Method for Medical and Biological Students*. London: George Allen and Unwin; 1940. pp. 33–40.
22. King GJ, Liu ZJ, Wang LL, Chiu IY, Whelan MF, Huang GJ. Effect of distraction rate and consolidation period on bone density following mandibular osteodistraction in rats. *Arch Oral Biol* 2003;**48**:299–308.
23. Shin JY, Liu ZJ, King GJ. Trabecular organization in mandibular osteodistraction in growing and maturing rats. *J Oral Maxillofac Surg* 2005;in press.
24. Williams BE, King GJ, Liu ZJ, Rafferty KL. Sequential histomorphometric analysis of regenerate osteogenesis following mandibular distraction in the rat. *Arch Oral Biol* 2005;in press.
25. Gibson GJ, Kohler WJ, Schaffler MB. Chondrocyte apoptosis in endochondral ossification of chick sterna. *Dev Dyn* 1995;**203**:468–76.
26. Zimmermann B. Occurrence of osteoblast necroses during ossification of long bone cortices in mouse fetuses. *Cell Tissue Res* 1994;**275**:345–53.
27. Hollinger J, Mayer MH. Bone Regenerate, Concept and Update. In: McCarthy JG, editor. *Distraction of the Craniofacial Skeleton*. New York: Springer; 1999. pp. 3–19.
28. Conners NA, Liu ZJ, Bollen AM, King GJ. Fractal analysis of the regenerate in mandibular distraction osteogenesis in rats. *J Dent Res* 2003;**82**:1214.
29. McCarthy JG, Stelnicki EJ, Mehrara BJ, Longaker MT. Distraction osteogenesis of the craniofacial skeleton. *Plast Reconstr Surg* 2001;**107**:1812–27.
30. Liu ZJ, Marshall CD, Herring SW, King GJ. Biomechanical properties of the regenerate following mandibular distraction in rats. *J Dent Res* 2003;**82**:1215.
31. Stewart KJ, Weyand B, van't Hof RJ et al. A quantitative analysis of the effect of insulin-like growth factor-1 infusion during mandibular distraction osteogenesis in rabbits. *Br J Plast Surg* 1999;**52**:343–50.
32. Okazaki H, Kurokawa T, Nakamura K, Matsushita T, Mamada K, Kawaguchi H. Stimulation of bone formation by recombinant fibroblast growth factor-2 in callotasis bone lengthening of rabbits. *Calcif Tissue Int* 1999;**64**:542–6.
33. Tavakoli K, Yu Y, Shahidi S, Bonar F, Walsh WR, Poole MD. Expression of growth factors in the mandibular distraction zone: a sheep study. *Br J Plast Surg* 1999;**52**:434–9.
34. Collin-Osdoby P, Rothe L, Bekker S, Anderson F, Huang Y, Osdoby P. Basic fibroblast growth factor stimulates osteoclast recruitment, development, and bone pit resorption in association with angiogenesis in vivo on the chick chorioallantoic membrane and activates isolated avian osteoclast resorption in vitro. *J Bone Miner Res* 2002;**17**:1859–71.
35. Iwasaki M, Nakahara H, Nakata K, Nakase T, Kimura T, Ono K. Regulation of proliferation and osteochondrogenic differentiation of periosteum-derived cells by transforming growth factor-beta and basic fibroblast growth factor. *J Bone Joint Surg Am* 1995;**77**:543–54.
36. Bronckers AL, Goei W, van Heerde WL, Dumont EA, Reutelingsperger CP, van den Eijnde SM. Phagocytosis of dying chondrocytes by osteoclasts in the mouse growth plate as demonstrated by annexin-V labelling. *Cell Tissue Res* 2000;**301**:267–72.
37. Taniwaki NN, Katchburian E. Ultrastructural and lanthanum tracer examination of rapidly resorbing rat alveolar bone suggests that osteoclasts internalize dying bone cells. *Cell Tissue Res* 1998;**293**:173–6.

Copyright of Orthodontics & Craniofacial Research is the property of Blackwell Publishing Limited and its content may not be copied or emailed to multiple sites or posted to a listserv without the copyright holder's express written permission. However, users may print, download, or email articles for individual use.